DOI: 10.1002/ange.200903201

Electronic Structure

Electromeric Rhodium Radical Complexes**

Florian Frank Puschmann, Jeffrey Harmer, Daniel Stein, Heinz Rüegger, Bas de Bruin, and Hansjörg Grützmacher**

Dedicated to Professor Martin Quack

Electromers are species with significantly different electronic but only slightly different geometrical structures, whereby each species corresponds to a local minimum on the energy hypersurface.[1a–c] Although they have been discussed several times in the literature, direct observation of "electroisomers"—the synonyms "redox isomers" or "valence isomers" are likewise used—is rare.[2] Paramagnetic transition-metal complexes are ideally suited to the study of this phenomenon, and the localization of the spin on either the metal M$^{\bullet}$(L) or the ligand M^{+}(L$^{\bullet-}$) can be characterized by EPR spectroscopy.[3] We report herein a striking example in which two electromers of paramagnetic rhodium complexes coexist in a rapid equilibrium and the distortion of only one P–Rh–P angle results in a substantial redistribution of the spin density.

We previously reported paramagnetic [M(tropp^{Ph})$_2$]^0 complexes (Scheme 1; M = Rh, Ir),[4a–d] which exist as rapidly exchanging *trans*/*cis* mixtures ($k_{isom} \approx 1 \times 10^4\ s^{-1}$) in solution. Both isomers have tetrahedrally distorted structures and their EPR spectra and consequently electronic structures are quite similar. They are best described as strongly delocalized organometallic radicals with less than 30 % of the spin density localized on the metal centers.[4e] We have now synthesized the rhodium complexes **5a**,**b**, which likewise contain two olefin and two phosphane binding sites in mutual *trans* positions, but the constraints within the ligand system do not allow *trans* to *cis* isomerization.

The syntheses of the ligand trop$_2$PPh **2** and the deep red complexes [Rh(trop$_2$PPh)(PPh$_3$)]$^+$A$^-$ (**5a**: A$^-$ = PF$_6^-$, **5b**: A$^-$ = BArF$^-$) are straightforward and proceed with excellent yields as shown in Scheme 1 (trop = 5H-dibenzo[*a*,*d*]-cycloheptene-5-yl). Exchange of the PF$_6^-$ anion by the BArF$^-$ anion (BArF$^-$ = tetrakis[(3,5-trifluoromethyl)phenyl]borate)[5] enhances significantly the solubility of **5b** (in diethyl ether, THF, or toluene). The structures of the ligand **2** and complex **5a** are shown in Figure 1.[6a,b] The rigid tripodal diolefin phosphane **2** is preorganized for binding a transition-metal ion in its cleft. Only a small rotation around the P–C$_{trop}$ bonds is necessary to convert **2** into the conformation it adopts in **5a**, explaining the high stability of this complex. As observed with the related amino ligand trop$_2$NH,[7] **5a** shows a distorted "sawhorse" (SH) type structure (a trigonal bipyramid with one missing edge in the equatorial plane):[8] the P1–Rh–P2 angle is 160.9° and the ct–Rh1–ct angle is 134.8° (ct = centroid of the coordinated C=C$_{trop}$ bond). The NMR data for all these complexes indicate that C_s-symmetrical SH-type structures are retained in solution and that there are no significant cation anion interactions (^{31}P nuclei in *trans* positions, inequivalent olefinic protons, superimposable data for **5a** and **5b**).

A cyclic voltammogram of **5a** in THF/1M *n*Bu$_4$N$^+$PF$_6^-$ shows two reversible waves at $E_1° = -1.339$ V and $E_2° =$

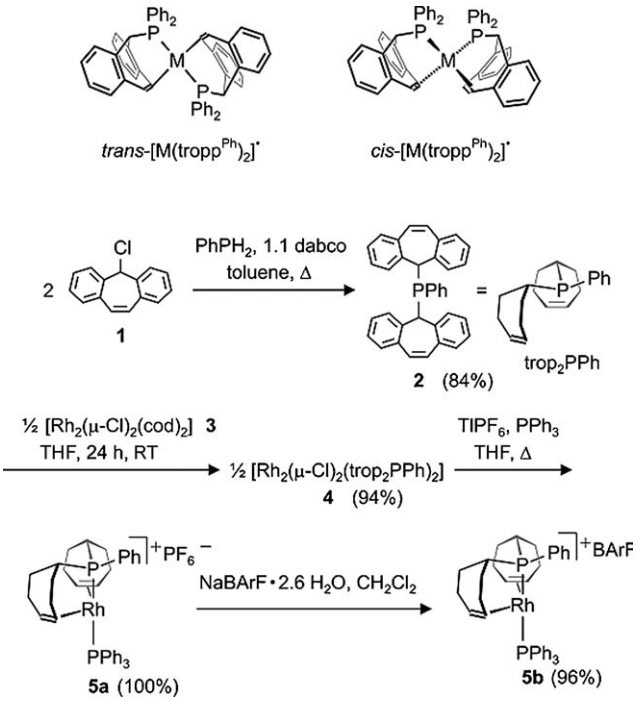

Scheme 1. Synthesis of trop$_2$PPh (**2**) and the Rh complexes **5a** and **5b**.

[*] Dipl.-Chem. F. F. Puschmann, Dr. D. Stein, Dr. H. Rüegger, Prof. Dr. H. Grützmacher
Department of Chemistry and Applied Biology
ETH-Hönggerberg, 8093 Zürich (Switzerland)
E-mail: gruetzmacher@inorg.chem.ethz.ch
Dr. B. de Bruin
Universiteit van Amsterdam, Faculty of Science
Van't Hoff Institute for Molecular Sciences, Homogeneous and Supramolecular Catalysis, Nieuwe Achtergracht 166
1018 WV Amsterdam (The Netherlands)
E-mail: b.debruin@uva.nl
Dr. J. Harmer
Inorganic Chemistry, University of Oxford (UK)

[**] This work was supported by the Swiss National Science Foundation (SNF), the Netherlands Organisation for Scientific Research (NWO-CW), the European Research Council (ERC Starting Grant 202886), the University of Amsterdam (UvA), and the ETH Zürich.

Supporting information for this article is available on the WWW under http://dx.doi.org/10.1002/anie.200903201.

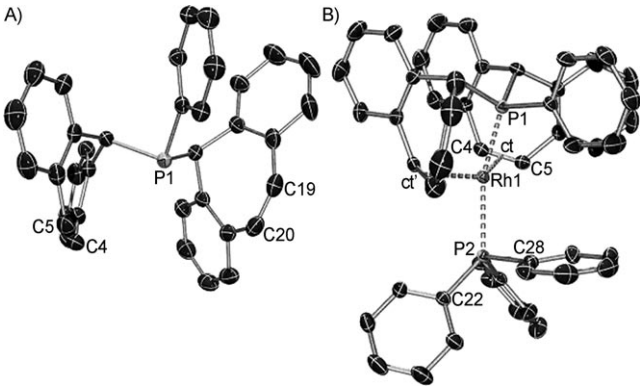

Figure 1. A) ORTEP plot (at 30% ellipsoid probability) showing the structure of **2**. Only one of the two crystallographically independent molecules is shown. Hydrogen atoms are omitted for clarity. Selected bond lengths [Å] and angles [°] (bond length of the second molecule are given in italics): C4=C5 1.338(3), *1.339(3)*, C19=C20 1.340(3), *1.343(3)*, Σ°(C-P-C) 300.7(2), *301.3(2)*. B) ORTEP plot (at 30% ellipsoid probability) showing the structure of the cation of **5a**·2 CH_2Cl_2. The PF_6^- anion, the CH_2Cl_2 solvent molecules, and hydrogen atoms are omitted for clarity. Selected bond lengths [Å] and angles [°]: Rh1–P1 2.231(1), Rh1–P2 2.359(1), Rh1–ct 2.099(3), Rh1–C4 2.194(3), Rh1–C5 2.233(3), C4=C5 1.405(4), Rh1–C22 3.712(5), Rh1–C28 2.905(4), P1-Rh1-P2 160.9(1), ct-Rh1-ct′ 134.8(2), Rh1-P2-C22 124.9(3), Rh1-P2-C28 87.0(2), Σ°(C-P1-C) 314.7(8), Σ°(C-P2-C) 317.2(7).

−1.965 V (vs. ferrocenium/ferrocene) for the redox couples $[Rh(trop_2PPh)(PPh_3)]^+/[Rh(trop_2PPh)(PPh_3)]^0$ and $[Rh(trop_2PPh)(PPh_3)]^0/[Rh(trop_2PPh)(PPh_3)]^{-1}$, respectively.

Chemically, **5b** can be reduced by one electron with elemental sodium, sodium naphthalide, or $[CoCp^*_2]$[9] (Cp* = 1,2,3,4,5-pentamethylcyclopentadienyl) in THF (Scheme 2). The EPR spectrum of the X band ($T = 120$ K) and W band ($T = 20$ K) of a frozen solution clearly supports two paramagnetic rhodium complexes **6L**• and **6M**• (Figure 2 A,B), which were fully characterized by high-resolution pulse EPR spectroscopy of the X, Q, and W bands (see the Supporting Information for details).[10] In contrast to the *cis*/*trans*-$[Rh(tropp^{Ph})_2]$• complexes (Scheme 1), which are highly persistent

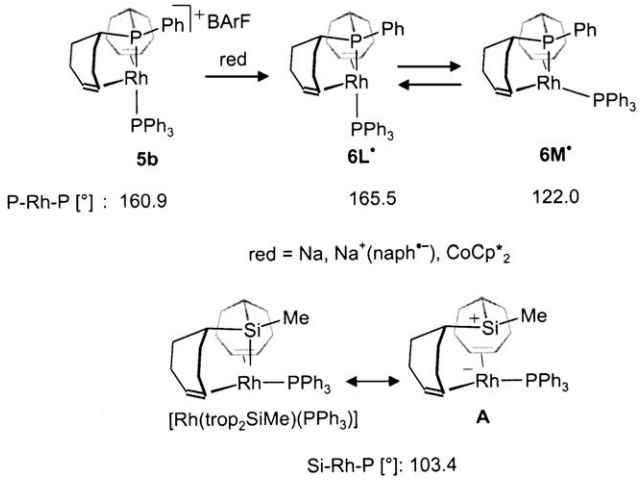

Scheme 2. Reduction of **5b** to give a mixture of **6L**• and **6M**•.

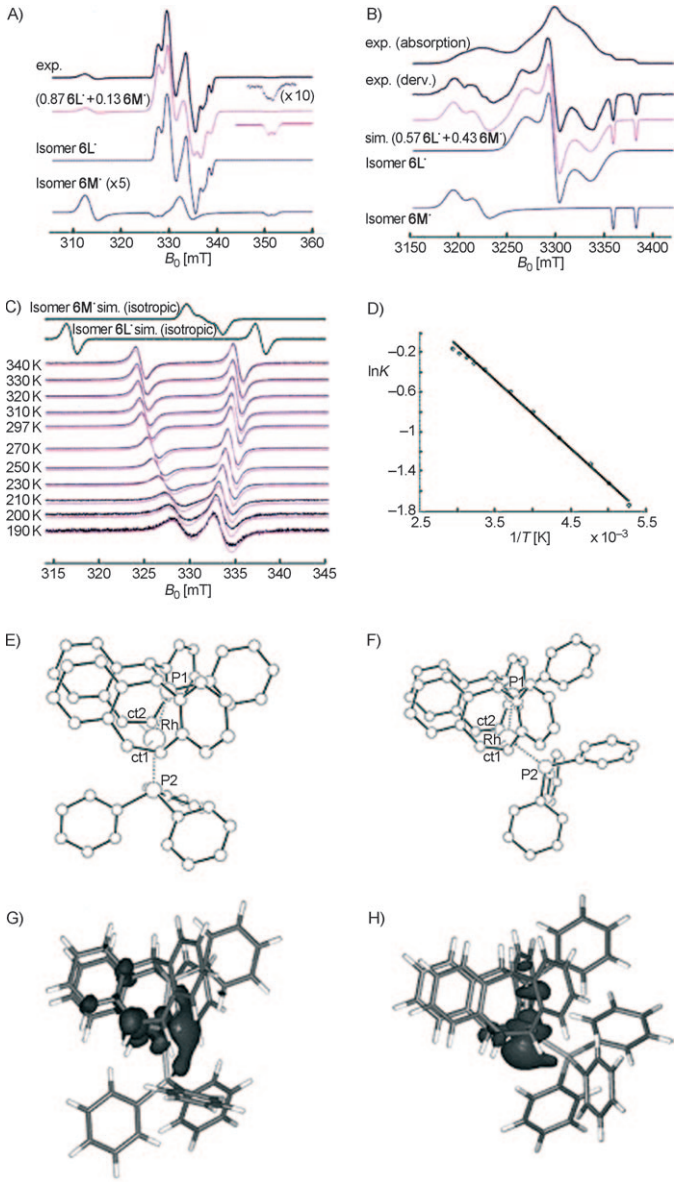

Figure 2. A) X-band (9.5065 GHz) continuous wave (CW) EPR spectrum of a mixture of **6L**• and **6M**• measured at $T = 120$ K in a toluene/THF mixture. The upper trace (black, bold) displays the experimental spectrum; the second trace (magenta) the simulated spectrum comprising 0.87 **6L**• + 0.13 **6M**•. The lower traces show the simulated EPR spectra of the single components. B) W-band (94.2947 GHz) FID-detected EPR spectrum measured at $T = 20$ K in a toluene/THF mixture. The *g* values of **6L**• were resolved at this microwave frequency. Isomer **6M**• displays an axial spectrum with a resolved doublet from a large ^{31}P hyperfine interaction. C) X-band (9.4793 GHz) CW EPR spectra of a mixture of **6L**• and **6M**• in THF recorded at $T = 190$–340 K. The simulated spectra describing the **6L**•⇄**6M**• ratios are displayed in magenta. D) Van't Hoff plot, $\ln(K_{eq})$ vs. $1/T$, for the ratio $K_{eq} = [\mathbf{6M}^\bullet]/[\mathbf{6L}^\bullet]$ from the simulation at each temperature in (C), used to evaluate the thermodynamic stabilities. E) Computed structure of **6L**•. Selected bond lengths [Å] and angles [°]: P1–Rh 2.259, P2–Rh 2.397, Rh–ct1 2.114, Rh–ct2 2.106, P1-Rh-P2 165.5, ct1-Rh-ct2 134.5. F) Computed structure of **6M**•. Selected bond lengths [Å] and angles [°]: P1–Rh 2.257, P2–Rh 2.444, Rh–ct1 2.097, Rh–ct2 2.094, P1-Rh-P2 122.0, ct1-Rh-ct2 131.2. G) Computed (b3-lyp, TZVP) spin density of **6L**•. H) Computed (b3-lyp, TZVP) spin density of **6M**•.

in solution, the radicals **6L**• and **6M**• react to give a mixture of diamagnetic products.[11]

The EPR spectra of the X band of the deep brown solutions in the temperature range 190–340 K are shown in Figure 2C. The changes in the spectra are fully reversible and indicate an equilibrium between two electronically different species that rapidly exchange on the EPR time scale (ca. 1 GHz).

The exchange process in solution is fast on the EPR time scale at all temperatures and only an averaged spectrum is observed. Lowering the temperature shifts the fast equilibrium **6L**•⇔**6M**• strongly towards **6L**• (the concentration of isomer **6L**• is approximately 66% at 340 K and 88% at 190 K). However, the very different electronic structure and therefore markedly different g values and hyperfine couplings of **6L**• and **6M**• render the averaged spectrum very sensitive to its temperature-dependent ratio. This behaviour allowed us to evaluate the equilibrium constant $\mathbf{6M}^{\bullet}/\mathbf{6L}^{\bullet} = K_{eq}$ at each temperature T through spectral simulation. The relative thermodynamic stabilities were estimated through a Van't Hoff plot ($\ln K_{eq}$ vs. $1/T$; Figure 2D). Accordingly, **6L**• is more stable than **6M**• by $\Delta H° = (-1.2 \pm 1)$ kcal mol^{-1} and $\Delta S° = (3.9 \pm 4)$ cal mol^{-1} K^{-1}. In agreement with the experimentally observed fast exchange process, DFT computations based on smaller models of **6L**• and **6M**• (see the Supporting Information) reveal a small energy barrier (ca. 3 kcal mol^{-1}).[12] Both species are detected in frozen solution upon rapid freeze-quenching with liquid nitrogen (i.e. under non-equilibrium conditions).

To gain insight into the electronic structures of **6L**• and **6M**•, we performed DFT calculations with the complete molecule [Rh(trop$_2$PPh)(PPh$_3$)]•. Table 1 lists the experimental and computed EPR data. Structure optimizations led to three stable species, which are close in energy. On the basis of comparison with the experimental data of **6L**• and **6M**•, these species are denoted as **6L**•$_{cal}$, **6L′**•$_{cal}$, and **6M**•$_{cal}$, respectively. The most- and least-stable isomers **6L**•$_{cal}$ ($E_{rel} = 0.0$ kJ mol^{-1}) and **6L′**•$_{cal}$ ($E_{rel} = +2.1$ kcal mol^{-1}), respectively, are rotamers obtained by rotation of the PPh$_3$ group (see the Supporting Information). Both have structures closely related to that of the cation of diamagnetic precursor **5a**.

The second most stable isomer **6M**•$_{cal}$ is 2.0 kcal mol^{-1} higher in energy than **6L**•$_{cal}$ and has a structure in which the P1–Rh–P2 angle closes from 165.5° to 122.0°. Concomitantly, the distance of Rh to the PPh$_3$ group becomes longer (Rh–P2 in **6L**•$_{cal}$: 2.397 Å; in **6M**•$_{cal}$: 2.444 Å). This result points to a shift of the electron density onto the metal on going from **6L**• to **6M**• (see below). Structure **6M**•$_{cal}$ approaches the extreme case of a trigonal pyramid, in which the P–Rh–P angle would be 90°. This structural feature was recently observed for the bistropsilyl complex [Rh(trop$_2$SiMe)(PPh$_3$)] for which we assumed—because of the strong σ-electron donation of the silyl group—a strong contribution of the resonance form **A** (Scheme 2) and enhanced electron density at the metal center.[13] A more detailed interpretation of the different electronic structures of **6L**• and **6M**• is given in the Supporting Information.

The computed EPR parameters of the lowest energy species **6L**•$_{cal}$ fit best to the experimental values of the more stable major isomer **6L**•, whereas the computed data for the somewhat higher energy species **6M**•$_{cal}$ are in good accord with the experimental values of the less abundant isomer **6M**• (Table 1). The experimental g_{iso} values of both isomers differ significantly from $g_e = 2.0023$ and indicate spin density at the metal center. In **6M**•, the larger anisotropy of the g tensor (**6L**•: $\Delta g = 0.043$; **6M**•: $\Delta g = 0.101$) shows that the spin density is higher at the Rh center. Note the large difference of the hyperfine couplings of the ^{31}P nucleus of the trop$_2$PPh ligand in **6M**• ($A^{P}_{iso} = (602 \pm 5)$ MHz) and **6L**• ($A^{P}_{iso} = (53 \pm 8)$ MHz), which demonstrate the very different electronic structure of both electromers. Our DFT computations support this picture. In **6L**•$_{cal}$, only 33% of the spin density is located at Rh, 12% at P1, and 9% at P2, with the residual spin density delocalized over the trop$_2$PPh and PPh$_3$ ligand. In **6M**•$_{cal}$, more than half of the spin density [ρ(Rh) 58%] is located at Rh. Another 28% resides on P1 and only 14% is delocalized over P2 [ρ(P2) 3%] and the hydrocarbon framework. Electromer **6L**• is best described as a strongly delocalized organometallic radical, whereas **6M**• should be considered as a metallo radical with a high localization of the spin density in the Rh–P1 bond.

In this report, we provide compelling evidence for the existence of interconverting and energetically almost degenerate organometallic electromers, which could be

Table 1: Experimental and DFT calculated (values in italics) g values, hyperfine coupling constants (A [MHz]), and spin densities ρ of compounds **6L**• and **6M**•.[a]

	6L• (major species detected in the experimental EPR spectra)				
exp		$g_{11} = 2.063 \pm 1$	$g_{22} = 2.043 \pm 1$	$g_{33} = 2.020 \pm 1$	$g_{iso} = 2.042 \pm 1$
calcd		*$g_{11} = 2.048$*	*$g_{22} = 2.035$*	*$g_{33} = 2.008$*	*$g_{iso} = 2.034$*
	ρ	A_{11}	A_{22}	A_{33}	A_{iso}
	–	22 ± 10	22 ± 10	115 ± 5	53
	12.2%	*22*	*27*	*70*	*40*
^{31}P2 exp	–	-56 ± 5	-50 ± 5	10 ± 15	-32
calcd	*9.0%*	*−7*	*−3*	*+24*	*+5*
^{103}Rh exp	–	17 ± 5	-17 ± 10	-32 ± 2	-10
calcd	*32.8%*	*+2*	*−20*	*−39*	*−19*
	6M• (minor species detected in the experimental EPR spectra)				
exp.		$g_{11} = 2.100 \pm 1$	$g_{22} = 2.100 \pm 1$	$g_{33} = 1.999 \pm 1$	$g_{iso} = 2.066 \pm 1$
calcd		*$g_{11} = 2.084$*	*$g_{22} = 2.078$*	*$g_{33} = 1.999$*	*$g_{iso} = 2.054$*
	ρ	A_{11}	A_{22}	A_{33}	A_{iso}
^{31}P1 exp	–	575 ± 5	575 ± 5	655 ± 5	602
calcd	*28.2%*	*457*	*459*	*601*	*506*
^{31}P2 exp	–		0 to −22		–
calcd	*3.1%*	*−35*	*−30*	*−10*	*−25*
^{103}Rh exp	–	24 ± 2	24 ± 5	-38 ± 2	3
calcd	*58%*	*26*	*18*	*−41*	*1*

[a] The signs of the experimental hyperfine couplings are assigned according to the DFT results.

detected through the observation of the paramagnetic rhodium complex $[Rh(trop_2PPh)(PPh_3)]^{\bullet}$ by EPR spectroscopy under ambient conditions. It remains to be explored how far the reactivity of the highly delocalized radical **6L**$^{\bullet}$ and the metalloradical **6M**$^{\bullet}$ can be distinguished.

Experimental Section

All manipulations were performed under an inert atmosphere of argon using standard Schlenk techniques. Selected analytical data are given below (see the Supporting Information for more details).

$trop_2PPh$ (**2**): trop-Cl (8.20 g, 36 mmol) and phenylphosphane (1.9 mL, 17.3 mmol) were dissolved in toluene (100 mL). 1,4-Diazabicyclo[2.2.2]octane (dabco) (3.87 g, 34.5 mmol) dissolved in toluene (200 mL) was added dropwise under vigorous stirring. The mixture was heated at reflux for 2 h, and dabco hydrochloride was filtered off while the mixture was still hot. The mixture was reduced in volume to 30 mL under reduced pressure, and the product crystallized within 12 h to give 7.11 g (14.5 mmol, 84%) of colorless microcrystals. ^{1}H NMR (300 MHz, CD_2Cl_2, 298 K): $\delta = 6.70$ (br d, $^3J_{HH} = 11.7$ Hz, 2H, H_{olefin}), 6.60 (br d, $^3J_{HH} = 11.7$ Hz, 2H, H_{olefin}), 4.53 ppm (br d, $^2J_{PH} = 3.6$ Hz, 2H, $2H_{benz}$); ^{13}C{^{1}H} NMR (75.5 MHz, CD_2Cl_2, 298 K): $\delta = 132.4$ (d, $^4J_{PC} = 5.1$ Hz, C_{olefin}), 131.7 (d, $^4J_{PC} = 4.3$ Hz, C_{olefin}), 55.6 ppm (d, $J_{PC} = 26$ Hz, C_{benz}); ^{31}P{^{1}H} NMR (121.5 MHz, CD_2Cl_2, 23 °C): $\delta = -7.0$ ppm; m.p.: 218 ± 2 °C.

$[Rh(PPh_3)(trop_2PPh)]PF_6$ (**5a**): $[Rh_2(\mu\text{-}Cl)_2(cod)_2]$ (105 mg, 0.212 mmol; cod = 1,5-cyclooctadiene) and $trop_2PPh$ (221 mg, 0.45 mmol) were dissolved in THF (15 mL). After several minutes, the solution changed color from yellow to orange and $[Rh_2(\mu\text{-}Cl)_2(trop_2PPh)_2]\cdot 1.5\,THF$ started to precipitate. After 1 day at T = 298 K, 271 mg (0.198 mmol, 94%) of the air stable product was collected as an orange microcrystalline powder. This product was dissolved in THF (40 mL) and heated at reflux for 12 h in the presence of PPh_3 (115 mg; 0.438 mmol) and $TlPF_6$ (210 mg; 0.601 mmol). Subsequently, the solvent was removed under reduced pressure, and the remaining red solid was treated with CH_2Cl_2 (150 mL). Insoluble material (TlCl) was filtered off over celite, and the filtrate was reduced in volume to 15 mL and layered with diethyl ether (50 mL) to give 400 mg (0.400 mmol, 100%) of **5a** as air-stable red microcrystals. ^{1}H NMR (400 MHz, CD_2Cl_2, 298 K): $\delta = 6.63$ (ddd, $^3J_{HH} = 8.8$ Hz, $^3J_{PH} = 4.0$ Hz, $^3J_{PH} = 4.0$ Hz, 2H, H_{ol}), 5.43 (ddd, $^3J_{HH} = 8.8$ Hz, $^3J_{HP} = 2.8$ Hz, $^3J_{HP} = 2.8$ Hz, 2H, H_{ol}), 5.31 ppm (dd, $^2J_{PH} = 14.6$ Hz, $^3J_{RhH} = 7.6$ Hz, $2H_{benz}$); ^{13}C{^{1}H} NMR (75.5 MHz, CD_2Cl_2, 298 K): $\delta = 90.3$ (d, $^1J_{RhC} = 10.8$ Hz, C_{ol}), 78.0 (d, $^1J_{RhC} = 4.8$ Hz, C_{ol}), 49.6 ppm (d, $^1J_{PC} = 15.9$ Hz, C_{benz}); ^{31}P{^{1}H} NMR (121.5 MHz, CD_2Cl_2, 23 °C): $\delta = 166.3$ (dd, $^1J_{RhP} = 145.2$ Hz, $^2J_{PP} = 327.6$ Hz, $trop_2PPh$), 24.4 (dd, $^1J_{RhP} = 107.0$ Hz, $^2J_{PP} = 327.6$ Hz, PPh_3), −144.06 ppm (sept, $^1J_{PF} = 714.5$ Hz, PF_6). mp: 238 ± 2 °C (decomposition); for a description of the anion exchange leading to **5b** see the Supporting Information.

Received: June 13, 2009
Revised: July 22, 2009
Published online: December 2, 2009

Keywords: EPR spectroscopy · radicals · redox chemistry · rhodium · valence isomerization

[1] a) We refer to the definition given by G. N. Lewis and G. T. Seaborg who in 1939 defined the term "electromer" as two forms of a molecule with the atoms in the same, or nearly the same, relative position but with a difference in electronic distribution. G. N. Lewis, G. T. Seaborg, *J. Am. Chem. Soc.* **1939**, *61*, 1886; for recent work, see: b) T. Bally, A. Maltsev, F. Gerson, D. Frank, A. de Meijere, *J. Am. Chem. Soc.* **2005**, *127*, 1983; c) B. Müller, T. Bally, F. Gerson, A. de Meijere, M. von Seebach, *J. Am. Chem. Soc.* **2003**, *125*, 13776.

[2] The observation of two or more forms of electromers has been especially achieved with complexes carrying "non-innocent" ligands, such as the semiquinone/catecholate pair, which are involved in intramolecular redox processes: $M^z(sq^{\bullet-}) \rightleftarrows M^{z+1}(cat^{2-})$: Reviews: a) E. Evangelio, D. Ruiz-Molina, *Eur. J. Inorg. Chem.* **2005**, 2957; b) P. Gütlich, A. Dei, *Angew. Chem.* **1997**, *109*, 2852; *Angew. Chem. Int. Ed. Engl.* **1997**, *36*, 2734; c) for an EPR study of paramagnetic Rh "redox isomers", see: B. V. Lebedev, N. N. Smirnova, G. A. Abakumov, V. K. Cherkasov, M. P. Bubnov, *J. Organomet. Chem.* **1989**, *485*, 341; d) for $Cu^I(Q^{\bullet-})/Cu^{II}(Q^{2-})$ "redox isomers" (Q = quinone type ligand), see: W. Kaim, M. Wanner, A. Knödler, S. Záliš, *Inorg. Chim. Acta* **2002**, *337*, 163, and references therein; e) for Pd complexes with benzonitroso ligands $Pd^{II}(R{-}N{=}O)/Pd^{I}(R{-}N{-}O^{\bullet})$, see: G. M. Larin, T. A. Stromnova, S. T. Orlova, *Russ. Chem. Bull. Int. Ed.* **2005**, *54*, 1798; f) for ligand-based "redox isomers" $Zn^{II}(L^{2-})(L^0)/Zn^{II}(L^{\bullet-})(L^{\bullet-})$, see: P. Chaudhuri, M. Hess, K. Hildenbrand, E. Bill, T. Weyhermüller, K. Wieghardt, *Inorg. Chem.* **1999**, *38*, 2781–2790; g) for an unspecified example that may involve a $Rh^{II}(dbt)/Rh^{I}(dbt^{\bullet-})$ equilibrium (dbt = *o*-dibenzodithiolato), see: C. A. Ghilardi, F. Laschi, S. Midollini, A. Orlandini, G. Scapacci, P. Zanello, *J. Chem. Soc. Dalton Trans.* **1995**, 531; for computational analysis of the multistate epoxidation of ethene by $[Fe^{III}O(por^{+})]$ and $[Fe^{IV}O(por)]$ "electromers" (por = porphyrin ligand), see: S. P. de Visser, F. Ogliaro, N. Harris, S. Shaik, *J. Am. Chem. Soc.* **2001**, *123*, 3037.

[3] For a Review covering Rh-, Ir-, Pd-, and Pt-based radicals, see: B. de Bruin, D. G. H. Hetterscheid, A. J. J. Koekoek, H. Grützmacher, *Prog. Inorg. Chem.* **2007**, *55*, Chapter 5.

[4] a) H. Schönberg, S. Boulmaâz, M. Wörle, L. Liesum, A. Schweiger, H. Grützmacher, *Angew. Chem.* **1998**, *110*, 1492; *Angew. Chem. Int. Ed. Angew. Chem. Int. Ed. Engl.* **1998**, *37*, 1423; b) H. Grützmacher, H. Schönberg, S. Boulmaâz, M. Mlakar, S. Deblon, S. Loss, M. Wörle, *Chem. Commun.* **1998**, 2623; c) S. Deblon, L. Liesum, J. Harmer, H. Schönberg, A. Schweiger, H. Grützmacher, *Chem. Eur. J.* **2002**, *8*, 601; d) F. Breher, H. Rüegger, M. Mlakar, M. Rudolph, S. Deblon, S. Boulmaâz, H. Schönberg, J. Thomaier, H. Grützmacher, *Chem. Eur. J.* **2004**, *10*, 641–653; e) B. de Bruin, J. C. Russcher, H. Grützmacher, *J. Organomet. Chem.* **2007**, *692*, 3167.

[5] N. A. Yakelis, R. G. Bergman, *Organometallics* **2005**, *24*, 3579.

[6] Crystal structure data: a) $trop_2PPh$ (**2**): Colorless, air-sensitive single crystals of **2** were obtained by slow diffusion of hexane into a THF solution of **2**; $C_{36}H_{27}P$; triclinic; space group $P\bar{1}$; a = 11.2327(5), b = 13.3384(6), c = 19.7300(9) Å, α = 106.945(1), β = 99.145(1), γ = 105.070(1)°; V = 2640.9(2) Å^3; Z = 4; ρ_{calcd} = 1.234 g cm^{-3}; crystal dimensions 0.52 × 0.47 × 0.22 mm^3; diffractometer Bruker SMART Apex with CCD area detector; $Mo_{K\alpha}$ radiation (0.71073 Å), 298 K, $2\Theta_{max}$ = 54.20°; 11483 reflections, 7889 independent (R_{int} = 0.0421); direct methods; empirical absorption correction SADABS (ver. 2.03); refinement against full matrix (versus F^2) with SHELXTL (ver. 6.12) and SHELXL-97; 667 parameters, $R1$ = 0.0410 and w$R2$ (all data) = 0.1053, max./min. residual electron density 0.294/−0.221 e Å^{-3}. All non-hydrogen atoms were refined anisotropically. The contribution of the hydrogen atoms, in their calculated positions, was included in the refinement using a riding model; b) $[Rh(trop_2PPh)(PPh_3)]PF_6\cdot 2\,CH_2Cl_2$ (**5a**): red single crystals were obtained by slow diffusion of hexane into a solution of **5a** in CH_2Cl_2; $C_{56}H_{46}P_3Cl_4F_6Rh$; orthorhombic; space group *Pnma*; a = 23.914(10), b = 12.033(8), c = 12.070(5) Å; V = 5205(4) Å^3; Z = 4; ρ_{calcd} = 1.494 g cm^{-3}; crystal dimensions 0.42 × 0.31 × 0.29 mm^3; diffractometer Bruker SMART Apex with CCD area detector; $Mo_{K\alpha}$ radiation (0.71073 Å), 298 K, $2\Theta_{max}$ = 56.52°; 6504 reflec-

tions, 5455 independent ($R_{int} = 0.0409$); direct methods; refinement against full matrix (versus F^2) with SHELXTL (ver. 6.12) and SHELXL-97; 337 parameters, $R1 = 0.0486$ and w$R2$ (all data) = 0.1406, max./min. residual electron density 1.207/ −0.678 e Å^{-3}. All non-hydrogen atoms were refined anisotropically. The contribution of the hydrogen atoms, in their calculated positions, was included in the refinement using a riding model. CCDC 706734 (**2**) and 706733 (**5a**) contain the supplementary crystallographic data for this paper. These data can be obtained free of charge from The Cambridge Crystallographic Data Centre via www.ccdc.cam.ac.uk/data_request/cif.

[7] a) P. Maire, T. Büttner, F. Breher, P. Le Floch, H. Grützmacher, *Angew. Chem.* **2005**, *117*, 6477; *Angew. Chem. Int. Ed.* **2005**, *44*, 6318; b) T. Zweifel, J.-V. Naubron, T. Büttner, T. Ott, H. Grützmacher, *Angew. Chem.* **2008**, *120*, 3289; *Angew. Chem. Int. Ed.* **2008**, *47*, 3245.

[8] The SH structure is proposed for the transient carbonyls $[M(CO)_4]$ (M = Fe, Ru, Os): a) M. Poliakoff, J. J. Turner, *J. Chem. Soc. Dalton Trans.* **1974**, 2276; b) P. L. Bogdan, E. Weitz, *J. Am. Chem. Soc.* **1989**, *111*, 3163; c) calculations: J. Li, G. Schreckenbach, T. Ziegler, *J. Am. Chem. Soc.* **1995**, *117*, 486; d) for stable d^8 $[RuL_4]$ complexes with SH structure, see: M. Ogasawara, D. Huang, W. E. Streib, J. C. Huffman, N. Gallego-Planas, F. Maseras, O. Eisenstein, K. G. Caulton, *J. Am. Chem. Soc.* **1997**, *119*, 8642, and references therein.

[9] N. G. Connelly, W. E. Geiger, *Chem. Rev.* **1996**, *96*, 877.

[10] A. Schweiger, G. Jeschke, *Principles of Pulse Electron Paramagnetic Resonance*, Oxford Press, Oxford, **2001**.

[11] These products and the mechanism leading to their formation is currently under investigation and will be published elsewhere.

[12] For the real (nonsimplified) molecules, this barrier could be somewhat higher because of steric reasons.

[13] D. Ostendorf, C. Landis, H. Grützmacher, *Angew. Chem.* **2006**, *118*, 5293; *Angew. Chem. Int. Ed.* **2006**, *45*, 5169.

